**Superalloys 2016: Proceedings of the 13th International Symposium on Superalloys**
*Edited by: Mark Hardy, Eric Huron, Uwe Glatzel, Brian Griffin, Beth Lewis, Cathie Rae, Venkat Seetharaman, and Sammy Tin*
***TMS (The Minerals, Metals & Materials Society), 2016***

# FULL FIELD MODELING OF THE ZENER PINNING PHENOMENON IN A LEVEL SET FRAMEWORK - DISCUSSION OF CLASSICAL LIMITING MEAN GRAIN SIZE EQUATION

B. Scholtes[1,2], D. Ilin[1], A. Settefrati[2], N. Bozzolo[1], A. Agnoli[3], M. Bernacki[1]

[1] Mines ParisTech, PSL Research University, CEMEF Centre de mise en forme des matériaux, CNRS UMR 7635, CS 10207 rue Claude Daunesse, 06904 Sophia Antipolis Cedex, France
[2] Transvalor SA, 694 avenue Docteur Maurice Donat, 06250 Mougins, France
[3] Snecma Gennevilliers, 171 boulevard Valmy, 92702 Colombes, France

Keywords: Zener pinning, level set, grain growth

## Abstract

The dragging effect exerted by second phase particles on grain growth in two-dimensional systems is investigated. Full field simulations were performed to highlight the influence of the size and the surface fraction of the precipitates on the limiting mean grain size. A modified version of the 2D classical Zener equation is finally proposed based on these numerical experiments. It is shown that the proposed model is in good agreement with other works from the literature.

## Introduction

It is well-known that precipitates act as obstacles to the displacement of the grain boundaries and may hinder grain growth. Under certain conditions, second phase particles (SPP) can also pin the microstructure, leading eventually to a limiting mean grain size (MGS), which is characteristic of the Zener pinning. This phenomenon is widely used by metallurgists to control the grain size during the forming process of many alloys, including superalloys. Predictive tools are then needed to model accurately this phenomenon and thus optimize the final in-use properties of the materials. Classical laws predicting the limiting MGS, noted $\langle R_f \rangle$, have the following form:

$$\langle R_f \rangle = K \frac{\langle r_p \rangle}{f^m}, \tag{1}$$

where $\langle r_p \rangle$ and $f$ are respectively the mean radius and volume (resp. surface in 2D) fraction of SPP. $K$ and $m$ are two parameters that fluctuate according to the assumptions made to obtain the equation [1]. Recently, Moelans et al. [2] proposed to consider the volume fraction of particles located at the grain boundaries $f_{gb}$ instead of $f$, because only these precipitates exert effectively a dragging effect on the grain boundaries. The Eq. 1 is thus reformulated as follows:

$$\langle R_f \rangle = K \frac{\langle r_p \rangle}{f_{gb}^m}, \tag{2}$$

In the following, only the expression given by Eq. 2 will be discussed.

There are many approaches to model the Zener pinning phenomenon at the polycrystal scale. Probabilistic voxel-based approaches such as Monte Carlo [3, 4, 5, 6, 7, 8] (MC) were the first to be developed. Due to the explosion of the computer capacities, deterministic approaches have become more popular in the last years. These methods do not rely on probabilistic laws and are therefore more precise, but also more greedy in terms of numerical requirements. Several authors have chosen to model explicitly the grain boundaries [9, 10] but these methods are hardly used in 3D, mainly because handling the complex topological events (grain shrinkage, nucleation...) is still an open issue. Recently more attention has been paid to other methods, in which the interfaces are implicitly represented by mathematical functions, like the phase-field (PF) [2, 11, 12, 13] and the level-set (LS) [14, 1] methods. These two approaches present the great advantage of avoiding the complex problems which come with the explicit tracking of the interfaces. Although the PF method lies on strong physical and thermodynamical fundations, its formulations introduces purely numerical parameters (like the grains boundary width). On the other hand, the LS method only requires measurable quantities which have a direct physical interpretation [15], but still needs to be developed in order to consider specific metallurgical mechanisms (twin interfaces, anisotropy...).

First efforts to model the Zener pinning phenomenon in a LS framework are actually quite recent [14, 1]. In [1], numerical investigations are proposed in order to quantify the influences of the size and surface fraction of the SPP on the limiting MGS. Interestingly, even if the

relevance of Eq. 2 comparatively to Eq. 1 was proved, quite surprising results were obtained concerning Eq. 2. It has thus been found that Eq. 2 can not predict exactly the limiting MGS in microstructures characterized by different grain/particle size ratios (see [1], Fig. 10), which could be a reason of the scatter of $(K;m)$ values reported in the literature. To our knowledge, it has never been proposed to improve the model of Eq. 2 based on the results of accurate and representative simulations at the polycrystal scale. However even if the LS approach used in the previous study was very precise (no assumption concerning Zener pinning phenomenon), the simulations were limited in terms of representativity (limited number of grains, limited mesh size) due to their colossal numerical costs (several weeks of computations for a 2D polycrystal of around 1400 grains). Moreover, serious numerical difficulties were then encountered in these simulations, especially for the reinitialization of the LS functions.

Recently, the numerical efficiency of the LS model has been drastically improved in order to deal with more representative microstructures. A new direct reinitialization algorithm [16] and an efficient recoloring scheme [15] enabling to perform optimized and coalescence-free simulations have been developed. These optimizations have been tested on pure grain growth (GG) without SPP in 2D and 3D and have permitted to reduce significantly the numerical requirements. In the present work, a numerical investigation of the Zener pinning phenomenon in two dimensions is proposed. More specifically, full field experiments are performed in order to discuss a typical model predicting the MGS.

## Numerical model

As mentioned above, the model considered in this paper works around a LS description of the interfaces in a finite element (FE) framework. A LS function $\psi$ is defined over a domain $\Omega$ as the signed distance function to the interface $\Gamma$ of a sub-domain $G$ of $\Omega$. The values of $\psi$ are calculated at each interpolation point (node in the considered P1 formulation) and the sign convention states $\psi \geq 0$ inside $G$ and $\psi \leq 0$ outside:

$$\forall t \begin{cases} \psi(x,t) = \pm d(x,\Gamma(t)), x \in \Omega, \\ \Gamma(t) = \{x \in \Omega, \psi(x,t) = 0\}, \end{cases} \tag{3}$$

where $d(.,.)$ corresponds to the Euclidean distance.

When considering pure grain growth, each LS interface is then displaced by solving the following partial differential equation:

$$\begin{cases} \dfrac{\partial \psi(x,t)}{\partial t} - M\gamma\Delta\psi(x,t) = 0, \\ \psi(x,t=0) = \psi^0(x), \end{cases} \tag{4}$$

where $M$ and $\gamma$ are the grain boundary (GB) mobility and energy, respectively.

One major drawback of the LS approach lies in the possible alteration of the metric property during the transport stage (*i.e.* $\|\nabla\psi\| \neq 1$). This is particularly problematic when a specific remeshing technique depending on the distance property is used at the interface [17]. In addition, the diffusive formulation of Eq. 4 is valid only if the function $\psi$ is locally a distance function. Finally, the condition number associated with our weak formulation (P1 interpolation, implicit method) depends largely on the regularity of the function $\psi$ [18].

The distance function must therefore be reinitialized at each time step to recover the metric property $\|\nabla\psi\| = 1$. In [1], this operation is performed by solving a set of Hamilton-Jacobi partial differential equations. It has been proved in [16] that this approach is inefficient in the considered polycrystalline context. Since this early work, a new direct and parallel reinitialization algorithm has been developed and incorporated in the present model [16]. The latter has been proven extremely fast and accurate. In this algorithm, the LS interface is firstly discretized into a collection of segments (respectively triangles in 3D) and the nodal values of the LS function are then updated by finding the nearest element in the collection and calculating the distance between the considered node and this nearest element. This method takes advantage of a space-partitioning technique using $k$-d tree and an efficient bounding box strategy enabling to maximize the numerical efficiency for parallel computations.

In addition to the previous reinitialization algorithm, a recoloring scheme detailed in [15] has also been introduced. It presents the great advantage of reducing significantly the number of LS functions needed to represent the polycrystal, and prevent any undesirable coalescence event by recoloring dynamically the grains during the simulation when it is needed. This new tool has also permitted to reduce the numerical costs associated with the present model and to increase its robustness. We refer the interested reader to [15] for additional details concerning the recoloring scheme.

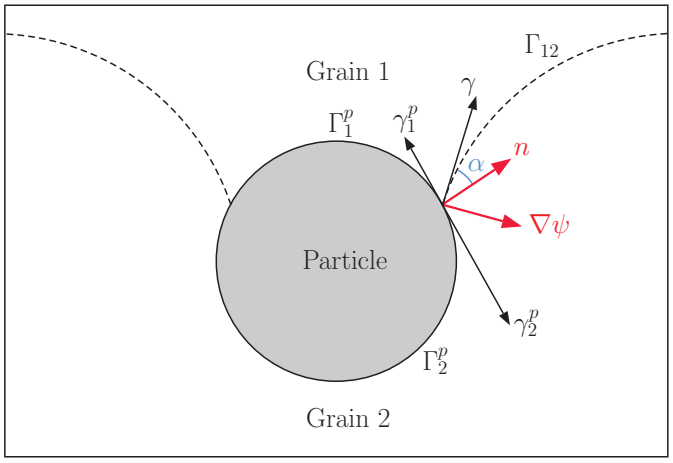


Figure 1: Scheme illustrating the SPP/GB interaction.

Handling of the grain boundary/particle interaction

The LS method is particularly interesting for the modeling of Zener pinning. Contrary to other numerical approaches, no assumption is required concerning the shape or the dragging force exerted by the SPP. The interaction angle $\alpha$ between the grain boundary (GB) and a precipitate is dictated by the balance of the surface tensions according to $\sin(\alpha) = (\gamma_2^p - \gamma_1^p)/\gamma$, where $\gamma_1^p$, $\gamma_2^p$ and $\gamma$ are respectively the surface tensions associated with the interfaces $\Gamma_1^p$, $\Gamma_2^p$ and $\Gamma_{12}$ (see Fig. 1). This constraint can be simply imposed by the mean of a boundary condition in the considered LS framework:

$$\frac{\nabla\psi}{\|\nabla\psi\|} \cdot \overrightarrow{n} = \nabla\psi \cdot \overrightarrow{n} = \sin(\alpha). \quad (5)$$

When a GB passes through a particle, its shape thus adapts to satisfy Eq. 5, which modifies its local curvature and therefore its kinetics.

Coherent or incoherent SPP can thus be considered by applying the suitable boundary conditions. In the case of incoherent precipitates, one has $\gamma_1^p = \gamma_2^p = \gamma$ and $\alpha = 0°$, which corresponds to a normal interaction angle between the GB and the particles. This configuration corresponds to a null boundary condition in Eq. 5. In practice, the SPP are represented by voids in the FE mesh and the boundary condition defined by Eq. 5 is directly integrated in the weak formulation of the FE problem (see [1] for further details). With the exception of the particular FE mesh needed to model the SPP, simulate pure GG or GG with precipitates in a LS/FE framework is then strictly equivalent and requires no further adaptation.

Simulation parameters

All the simulations are performed on a linux cluster (Xeon 1.2 GHz). On average, 16 CPUs are used for the simulations and the calculation times are around one or two days, depending on the configuration, which is considerably less than the ones from the previous study [1]. Furthermore, around twice as many grains are now considered, which enables more statistically representative predictions by limiting the impact of the edge effects.

The initial polycrystal follows the grain size distribution measured experimentally in Inconel 718. The values of the GB mobility and energy are respectively fixed to $M = 2.3 \times 10^{-23}\mathrm{m}^4/(\mathrm{Js})$ and $\gamma = 0.6\mathrm{J/m}^2$, which is representative of this material at a sub-solvus temperature (around 985°C) [1]. The simulated domain is a square with dimensions $0.3 \times 0.3\mathrm{mm}^2$, leading to an initial number of grains close to 2600. The initial MGS is $\langle R_0 \rangle = 3.35\mu$m. All SPP are perfectly circular with identical radius $r_p$ and assumed incoherent ($\alpha = 0°$ in Eq. 5).

Several tests have been performed in order to propose an adequate value for the time step and it has been observed that $\Delta t = 0.1$s is optimal for the considered problem.

## Results and discussion concerning the limiting mean grain size equation

The initial FE meshes with voids are generated using a frontal/Delaunay algorithm. In order to keep a high accuracy for the GB description, a metric-based *a posteriori* remeshing technique is employed to refine the mesh around the interfaces. The remeshing operations are performed by the mesher/remesher MTC [19]. The Fig. 2 illustrates a FE mesh, where it can be seen that elements are highly anisotropic and refined in the direction normal to the GB.

In the following, the results of the LS simulations are constantly confronted with the work of Moelans et al. [2]. In this study, PF simulations are performed to calibrate the Zener-type equation of Eq. 2 for different particle and grain sizes. As these results show good agreement with experimental observations, it is assumed they stand for a reliable comparison.

In the present study, four particle radii $r_p$ are tested ($0.2\mu$m, $0.4\mu$m, $0.8\mu$m and $1\mu$m) with surface fractions of 1% to 8%. For each simulation, the values of $f_{gb}$ and $\langle R_f \rangle$ are measured at the steady state (when

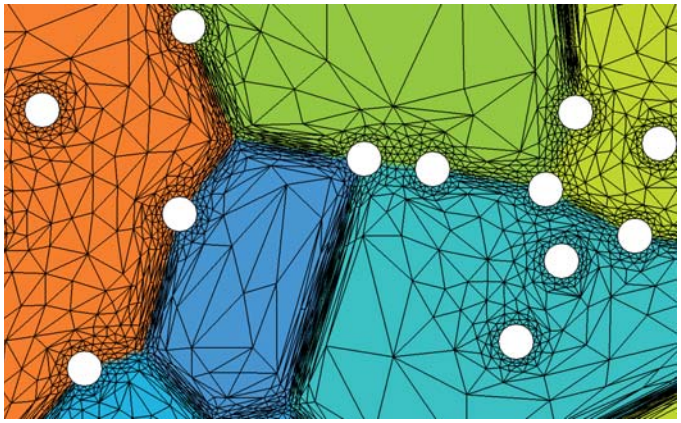

Figure 2: View of a FE mesh used for the Zener pinning simulations. The voids in the mesh (white disks) represent the SPP.

the MGS becomes stable). The Fig. 3 illustrates the microstructure for the configuration $r_p = 0.4\mu$m / $f = 3\%$ at the early and final stages of the simulation.

The evolution of the MGS during the heat treatment for different pinning configurations is plotted in Fig. 4. It appears that, for a given surface fraction, the radius of the precipitates influences drastically the GG kinetics. For example, with $r_p = 1\mu$m, 20min are needed to reach the steady state while the MGS becomes globally stationary after less than 5min with $r_p = 0.2\mu$m. The Fig. 5 summarizes the results obtained at steady state for all the simulated configurations.

As previously observed by Agnoli et al., all the data plotted in Fig. 5 can not be represented by a single master curve, which corroborates the idea that the formalism of Eq. 2 must be enhanced to predict the limiting MGS in microstructures presenting different grain/SPP size ratio. For this purpose we plot in Fig. 6 the evolution of the parameters $K$ and $m$ of Eq. 2, obtained with the present LS simulations, as a function of the initial grain/SPP size ratio. It is obvious that this normalization makes sense only for microstructure wherein the grain size distribution is relatively regular (relatively small deviation from the MGS), which is the case in the considered Inconel 718 material.

By using power regressions for these two parameters, the two following expressions are obtained:

$$K = \frac{0.362}{(r_p/\langle R_0\rangle)} \qquad \text{and} \qquad m = 0.853(r_p/\langle R_0\rangle)^{0.428}. \tag{6}$$

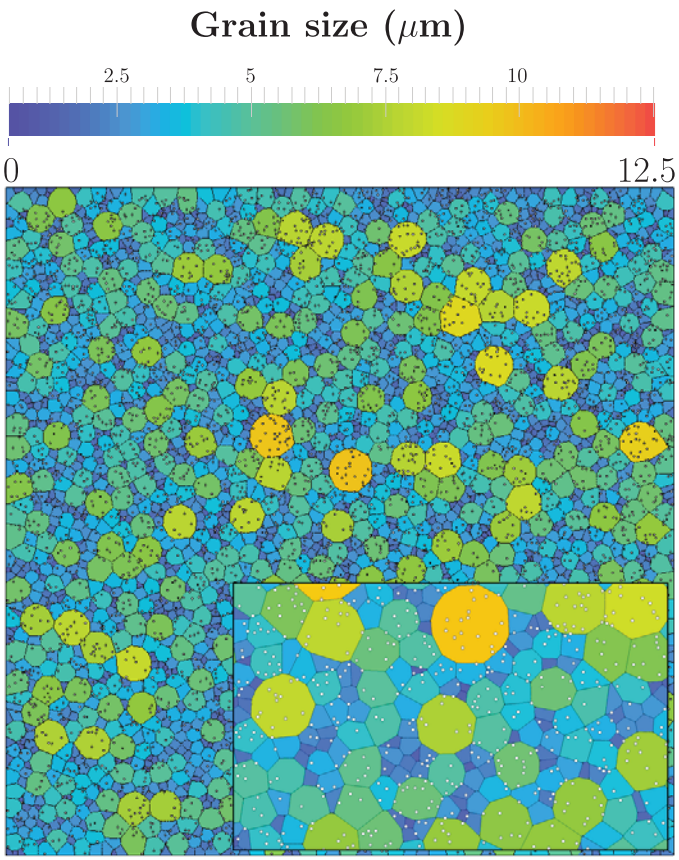


(a) $t = 0$

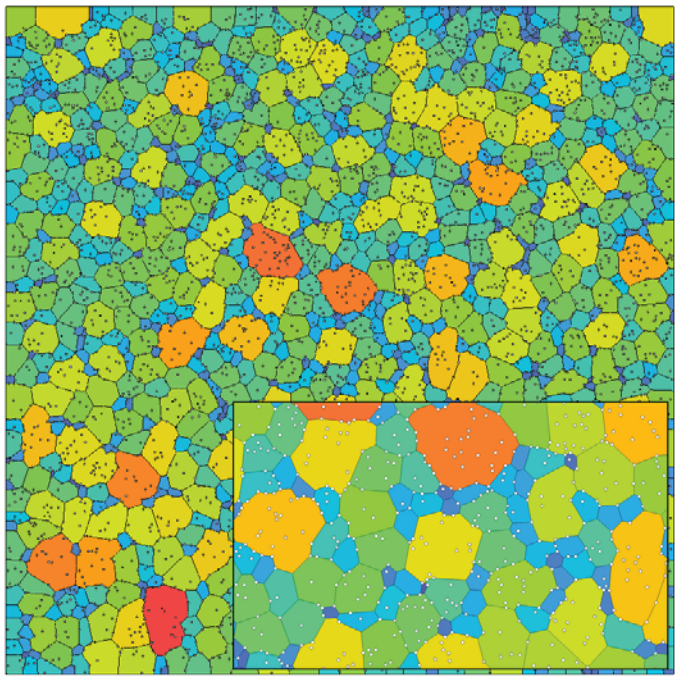

(b) $t = 9$min

Figure 3: Microstructure at the early and final stage of the simulation for the configuration $r_p = 0.4\mu$m / $f = 3\%$. The color code corresponds to the grain size.

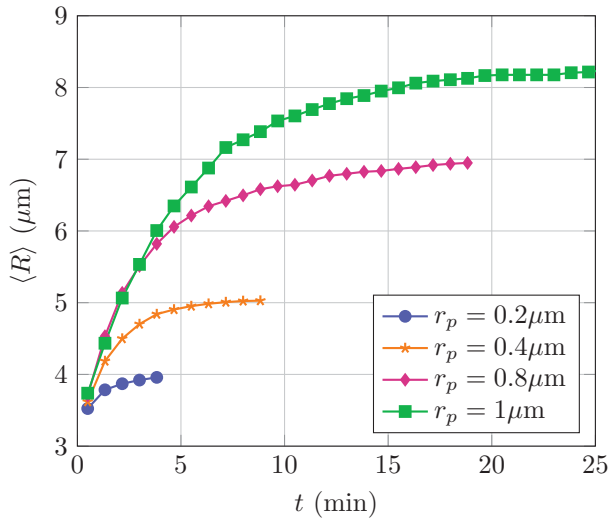


Figure 4: Evolution of the MGS during the heat treatment for different particle radii with a surface fraction $f = 3\%$.

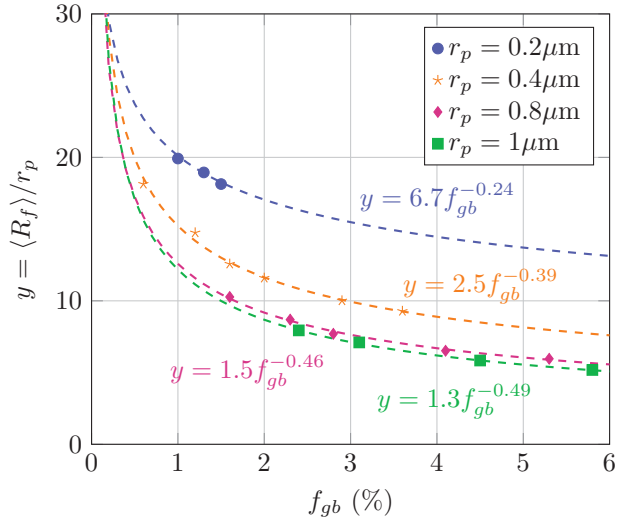


Figure 5: Results of the LS simulations measured at the steady state. Each dashed line corresponds to the best fit satisfying Eq. 2 for a given particle radius.

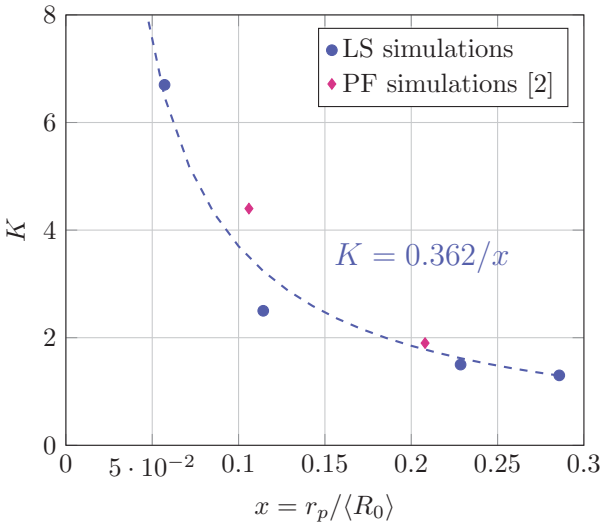


(a)

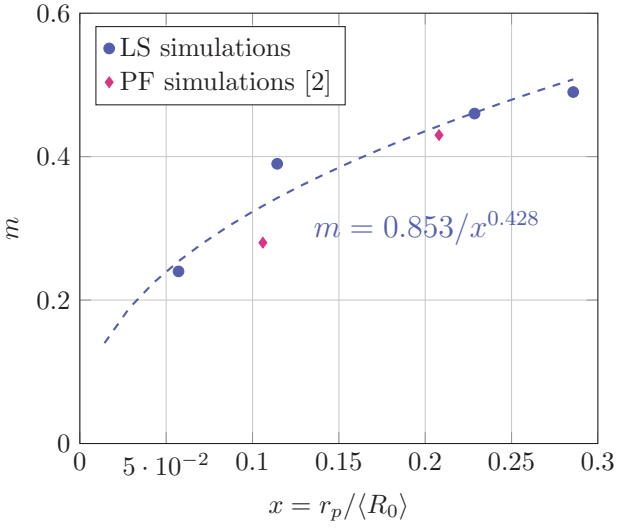


(b)

Figure 6: Values of $K$ and $m$ (see Eq. 2) obtained with full field simulations. The dashed lines correspond to the best power fits resulting from the LS simulations. Diamond data points are taken from [2].

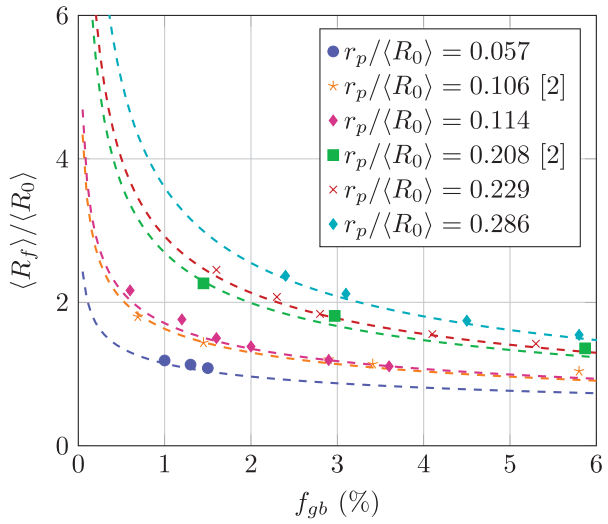


Figure 7: Predictions on the limiting MGS obtained with the model of Eq. 7 (represented by the dashed lines) for different SPP/grain size ratio and comparison with the results of full field simulations (LS and PF simulations [2]).

As illustrated in Fig. 6, the PF results of [2] fall very close from the trend lines obtained through the LS simulations, which tends to validate these results.

By replacing $K$ and $m$ in Eq. 2 with the expression of Eq. 6, the following expression is finally obtained for the limiting MGS:

$$\langle R_f\rangle = 0.362\langle R_0\rangle f_{gb}^{-0.853(r_p/\langle R_0\rangle)^{0.428}}. \qquad (7)$$

Fig. 7 illustrates the quality of the proposed model comparatively to the obtained LS results and the PF simulations of [2].

Although these results are quite satisfying, they shall obviously be substantiated with additional experimental validations. The 3D aspect must also be considered, as the real interaction between a GB and a particle can only be described in three dimensions. Thanks to the recent numerical improvements of the LS/FE model, 3D simulation of Zener pinning is now possible [15] (see Fig. 8) but computational times are still too elevated to enable the same type of study presented in this paper in three dimensions. Moreover, it appears important to investigate the variability of the fitting parameters of the new model (see Eq. 7). More precisely, it has been found in this study that the proposed values are in good agreement with the results of Moelans et al. [2] even if the material (grain size distribution, GB energy/mobility) and the thermal treatment conditions are different. This new model seems therefore quite

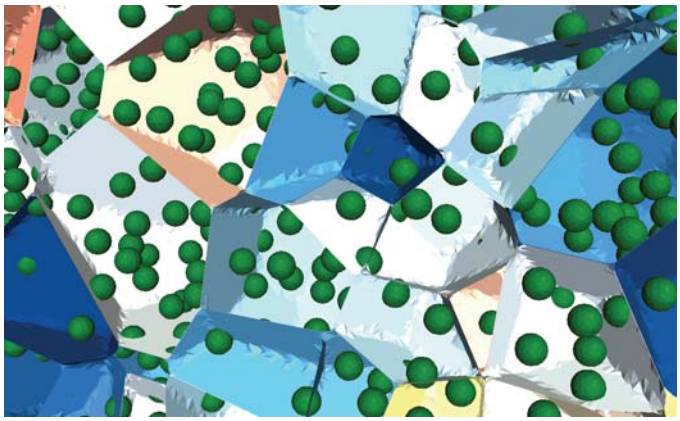

(a)

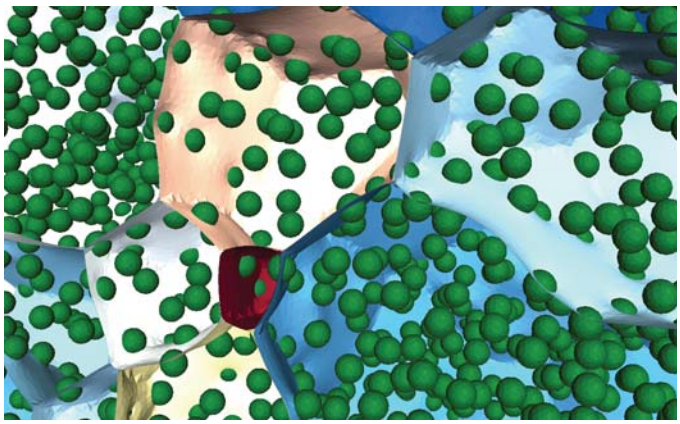

(b)

Figure 8: 3D simulation of GG with SPP in 3D. The Green spheres represent the precipitates.

generalizable. Further investigations should nevertheless be conducted in order to corroborate these first remarks. Finally, the enrichment of this mean field equation in order to consider more realistic microstructures (anisotropy of the GB energy, presence of twin boundaries...) is an interesting perspective.

## Conclusions

A set of 2D full field simulations of grain growth in Inconel 718 with second phase particles have been performed. Different particle clouds are tested in order to highlight and quantify the effects of the particle size and the surface fraction on the limiting mean grain size. The simulations have demonstrated that the classical Zener law can not predict accurately the limiting mean grain size at the steady state for every grain/particle size ratio. The parameters of this equation, which are assumed constant for stable thermomechanical conditions in the classical formulation, have then been expressed as func-

tions of the microstructure features (initial mean grain size and particle radius). Based on these numerical experiments, a new model of Zener pinning is finally proposed which shows very good agreement with reference works from the literature.

## References


[1] A. Agnoli, N. Bozzolo, R. Logé, J. Franchet, J. Laigo, and M. Bernacki, "Development of a level set methodology to simulate grain growth in the presence of real secondary phase particles and stored energy Application to a nickel-base superalloy," *Computational Materials Science*, vol. 89 (2014), 233–241.

[2] N. Moelans, B. Blanpain, and P. Wollants, "Phase field simulations of grain growth in two-dimensional systems containing finely dispersed second-phase particles," *Acta Materialia*, vol. 54 (2006), 1175–1184.

[3] D. Srolovitz, M. Anderson, G. Grest, and P. Sahni, "Computer simulation of grain growth - III. Influence of a particle dispersion," *Acta Metallurgica*, vol. 32 (9) (1984), 1429–1438.

[4] M. Anderson, G. Grest, R. Doherty, K. Li, and D. Srolovitz, "Inhibition of grain growth by second phase particles : Three dimensional Monte Carlo computer simulations," *Scripta Metallurgica*, vol. 23 (1989), 753–758.

[5] G. Hassold, E. Holm, and D. Srolovitz, "Effects of particle size on inhibited grain growth," *Scripta Metallurgica et Materialia*, vol. 24 (1990), 101–106.

[6] J. Gao, R. Thompson, and B. Patterson, "Computer simulation of grain growth with second phase particle pinning," *Acta Materialia*, vol. 45 (1997), 3653–3658.

[7] B. Kad and P. Hazzledine, "Monte Carlo simulations of grain growth and Zener pinning," *Materials Science and Engineering: A*, vol. 238 (1997), 70–77.

[8] K. Phaneesh, A. Bhat, P. Mukherjee, and K. Kashyap, "On the Zener limit of grain growth through 2D Monte Carlo simulation," *Computational Materials Science*, vol. 58 (2012), 188–191.

[9] S. Weygand, Y. Brechet, and J. Lépinoux, "Zener pinning and grain growth : A two-dimensional vertex computer simulation," *Acta Materialia*, vol. 47 (3) (1999), 961–970.

[10] G. Couturier, R. Doherty, C. Maurice, and R. Fortunier, "3D finite element simulation of the inhibition of normal grain growth by particles," *Acta Materialia*, vol. 53 (2005), 977–989.

[11] K. Chang, W. Feng, and L. Chen, "Effect of second-phase particle morphology on grain growth kinetics," *Acta Materialia*, vol. 57 (2009), 5229–5236.

[12] K. Chang and N. Moelans, "Phase-field simulations of the interactions between a grain boundary and an evolving second-phase particle," *Philosophical Magazine Letters*, vol. 95 (4) (2015), 202–210.

[13] M. Tonks, Y. Zhang, A. Butterfield, and X. Bai, "Development of a grain boundary pinning model that considers particle size distribution using the phase field method," *Modelling and Simulation in Materials Science and Engineering*, vol. 23 (4) (2015), 045009.

[14] A. Agnoli, M. Bernacki, R. Logé, J. Franchet, J. Laigo, and N. Bozzolo, "Understanding and modeling of grain boundary pinning in Inconel 718," *Superalloys 2012*, ed. E.S. Huron, et al, (Seven Springs, PA:TMS, 2012), 73–82.

[15] B. Scholtes, M. Shakoor, A. Settefrati, P.-O. Bouchard, N. Bozzolo, and M. Bernacki, "New finite element developments for the full field modeling of microstructural evolutions using the level set method," *Computational Materials Science*, vol. 109 (2015), 388–398.

[16] M. Shakoor, B. Scholtes, P.-O. Bouchard, and M. Bernacki, "An efficient and parallel level set reinitialization method - Application to micromechanics and microstructural evolutions," *Applied Mathematical Modelling*, vol. 39 (23-24) (2015), 7291–7302.

[17] D. Quan, T. Toulorge, E. Marchandise, J. Remacle, and G. Bricteux, "Anisotropic mesh adaptation with optimal convergence for finite elements using embedded geometries," *Computer Methods in Applied Mechanics and Engineering*, vol. 268 (2014), 65–81.

[18] M. Bernacki, Y. Chastel, T. Coupez, and R. Logé, "Level set framework for the numerical modelling of primary recrystallization in polycrystalline materials," *Scripta Materialia*, vol. 58 (2008), 1129–1132.

[19] T. Coupez, H. Digonnet, and R. Ducloux, "Parallel meshing and remeshing," *Applied Mathematical Modelling*, vol. 25 (2000), 153–175.